Vortex clusters in a stirred polariton condensate

I. Gnusov [1,*] S. Harrison [2] S. Alyatkin [1] K. Sitnik [1] H. Sigurðsson [3,4] and P. G. Lagoudakis [1]

[1]*Skolkovo Institute of Science and Technology, Moscow, Territory of innovation center "Skolkovo", Bolshoy Boulevard 30, bld. 1, 121205, Russia*

[2]*School of Physics and Astronomy, University of Southampton, Southampton, SO17 1BJ, United Kingdom*

[3]*Institute of Experimental Physics, Faculty of Physics, University of Warsaw, ul. Pasteura 5, PL-02-093 Warsaw, Poland*

[4]*Science Institute, University of Iceland, Dunhagi 3, IS-107 Reykjavik, Iceland*

(Received 18 August 2023; accepted 5 February 2024; published 12 March 2024)

Recently, we realized the formation of a single quantized vortex in nonresonantly optically stirred exciton-polariton condensates [I. Gnusov *et al.*, Sci. Adv. **9**, eadd1299 (2023)]. In this work, we demonstrate that the number of emerging vortices depends on the characteristic size of the rotating potential induced by the nonresonant laser excitation. For smaller sizes, we observe only a single vortex with a topological charge of ± 1 defined by the stirring direction. For larger trap sizes, clusters of up to four corotating vortices are observed, also following the stirring direction. We find that the interplay of stirring speed and confining potential size dictates the number of vortices in a cluster. This is confirmed by observed energy distribution of condensed polaritons as a function of rotation frequency. Our findings offer an insight into the behavior of stirred condensates, complementing previous works on optically trapped polariton condensates in static traps.

DOI: 10.1103/PhysRevB.109.104503

I. INTRODUCTION

The emergence of quantized vorticity in rotating, or "stirred," quantum fluids is a well-known hallmark of superfluidity. Classical experiments with stirred superfluid Helium [1,2] and Bose-Einstein condensates in ultracold atomic gases [3–5] showcased that vortices start appearing above a critical rotation speed and would grow proportionally with the rate of stirring. In such systems, the vortices self-arrange to form organized clusters like the energy-favorable triangular geometry [1,4,6]. Only recently was quantized vorticity reported in an optical platform which implemented a new form of a rotating environment, a nonresonantly optically stirred condensate of exciton polaritons [7,8]. This recent development opened a new pathway to explore spontaneous onset of polariton vorticity in which the direction of orbital angular momentum could be steered in a dynamically driven fashion [9,10].

Exciton-polaritons (further on polaritons) are bosonic quasiparticles that arise due to the strong coupling of the excitons and photons in semiconductor microcavities [11]. Many of their properties can be controlled through optical means, and can be measured via their photonic decay channel as photons escape the cavity. This makes polaritons a good playground to study many-body physics and macroscopic coherent quantum phenomena driven far from equilibrium. A polariton condensate [12,13] is a many-body coherent state described by a macroscopic wavefunction which reveals signatures of superfluidity and vorticity under certain external driving (excitation) conditions [14–16]. From the first experimental observation of quantized polariton vortices in 2008 [17], their study has been thriving to date with reports on half-quantized vortices [18,19], optically trapped vortices [20–24], vortex-antivortex pairs [25], oscillating vortex clusters [26], high charge vortices [27,28], chains [29,30] and lattices [31–35], and turbulent flows [36–38]. Aside from fundamental interests, polariton vorticity could play a role in practical devices either aimed at simulating spin systems [34], topological physics [39–41], or for unconventional [42] and quantum based computing [43,44].

Although the first observation of polariton vorticity was reported almost 15 years ago [17], it was only recently that experiments with stirred polariton fluids using nonresonant laser light were implemented [7,8]. In these recent experiments, a "rotating bucket" analog—of sorts—was designed for the polariton condensate leading to quantized vorticity, in a similar spirit to emblematic experiments on rotating superfluid helium [1] and ultracold atoms [5]. The reason for the delay in developing a rotating vessel experiment for polaritons is the extremely high and experimentally elusive GHz rotation speeds [7,8] required to stir the condensate because of the polariton's small effective mass (four orders of magnitude smaller than the free electron mass).

In these recent experiments, coherence and vorticity formed spontaneously for the stirred polaritons around condensation threshold, in sharp contrast to experiments where vorticity was optically imprinted either through parametric [16] or resonant [29,32] pumping. However, the inherent driven-dissipative nature of polaritons leads to very different physics when it comes to rotation [7,8] as compared to conservative (nonpumped) quantum fluids. The most striking difference is the collapse of the polariton condensate into a vortex-free state with increasing stirring frequency, whereas

*ivan.gnusov@skoltech.ru

in conventional quantum fluids one would see an increasing number of self-organized vortices [1,5].

Here, we map out this unique angular momentum ejection behavior of the stirred polariton fluid as a function of excitation parameters. We find that the number of vortices scales with the rotating optical trap size (diameter) and demonstrates clusters of up to four corotating vortices. The vortex clusters appear only in a narrow range of GHz stirring frequencies. This is corroborated by measurements on the statistical occurrence of the vortices as a function of rotation frequency. At a fixed stirring frequency, we reveal a transition from two corotating vortices to a single vortex with increasing excitation laser power. All of the observed vortex clusters display corotating vortices whose rotation direction is always dictated by the pump's stirring direction. Moreover, the energy spectrum of the stirred condensate is also found to depend strongly on the pump's rotation speed. Our experimental observations are supported by numerical mean field simulations using the generalized Gross-Pitaevskii equation.

II. RESULTS

The experiments were carried out using an inorganic 2λ $GaAs/AlAs_{0.98}P_{0.02}$ planar microcavity with embedded $In_{0.08}Ga_{0.92}As$ quantum wells [45]. The sample is held in the cryostat at 4K and excited nonresonantly with two excitation lasers each detuned by ≈ 100 meV from the lower polariton branch. The continuous wave (CW) lasers are chopped with an acoustooptic modulator to form 2 µs pulses to reduce the sample heating (see Sec. S1 of the Supplemental Material for details [46]). The cavity photon mode is negatively detuned from the exciton level by ≈ -3 meV. In order to optically induce the time-periodic rotating potential for polaritons, we utilize the technique described in Ref. [7]. In brief, the two single-mode lasers are frequency-stabilized and slightly detuned from one another, with frequencies $f_1 \neq f_2$. The lasers are spatially shaped using two reflective spatial light modulators (SLMs) in the form of "perfect vortex" beams of opposite orbital angular momentum [47]. Thus, the transverse profile of each beam is a ring with a winding phase profile about the beam axis (see experimental pump profiles in the Sec. S2 in the Supplemental Material [46]).

With the SLMs, we can independently control each beams' diameter d (i.e., the diameter of the annular ring-profile focused on the cavity plane) and optical angular momentum l. Specifically, we imprint the $l_{1,2} = \pm 1$ for the first and the second laser beam, respectively, or vice versa. Then, the two annular beams are spatially overlapped, forming a profile of broken axial symmetry, and focused onto the sample [see Fig. 1(a)]. The difference in frequencies of each beam $\Delta f = f_1 - f_2 \neq 0$ results in time-periodic interference causing the net profile to rotate at the frequency f in the plane of the cavity. The rate of rotation is given by [7,48]

$$f = \frac{\Delta f}{\Delta l} = \frac{f_1 - f_2}{l_1 - l_2}. \tag{1}$$

The sign of f defines the rotation direction of the total beam profile with anticlockwise and clockwise corresponding to positive and negative f, respectively.

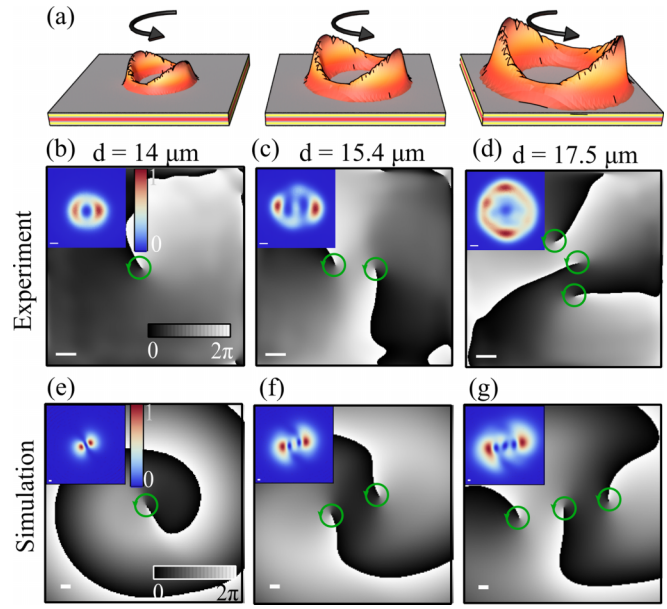

FIG. 1. (a) Schematic demonstrating three rotating optical traps (yellow to orange color scale) of different sizes. Experimentally measured real-space phase distribution of the condensate in the rotating trap with diameter of (b) 14 µm, (c) 15.4 µm, and (d) 17.5 µm. The insets in (b)–(d) show the time-integrated condensate intensity distribution. (e)–(g) Corresponding simulated instantaneous real-space phases with insets in panels, depicting the snapshots of the condensate intensity distribution. The scale bars in (b)–(g) equals 2 µm.

The rotating excitation beam first photoexcites a cloud of quantum well charge carriers which then relax in energy to form a reservoir of so-called bottleneck excitons which provide gain to the condensate through stimulated scattering [12]. Because of the strong repulsive Coulomb interactions between excitons and polaritons, the reservoir also leads to strong local blueshift which underpins the optical trapping mechanism of polaritons [49]. Therefore, at the mean field level, the exciton reservoir can be regarded as a time-dependent complex-valued potential for polariton waves.

Because of the finite lifetime of reservoir excitons the rotating beam profile induces a complex-valued potential that can be decomposed into a static part, referred to as the trap, and a rotating part which exerts torque on the polariton condensate [7] [see Fig. 1(a)]. The size and depth of the optical trap can be tuned through the diameter and power of the optical beam, respectively. These parameters define the number of accessible energy levels within the trap (i.e., confined modes) which condensate can occupy [50]. Indeed, because of its driven-dissipative nature, polaritons can condense into one or more higher energy trap levels due to intricate balance of gain and dissipation [50].

For the smallest optical trap with a diameter $d = 14$ µm rotated at $f = 2$ GHz, we observe a single quantized vortex, the same as in Ref. [7], corresponding to the condensate getting stirred into the trap's first excited state manifold [see Fig. 1(b)]. The condensate real-space phase distribution is measured with a homodyne interferometry technique [51]. The blue-red colored insets denote the real-space cavity photoluminescence (PL) which is proportional to the

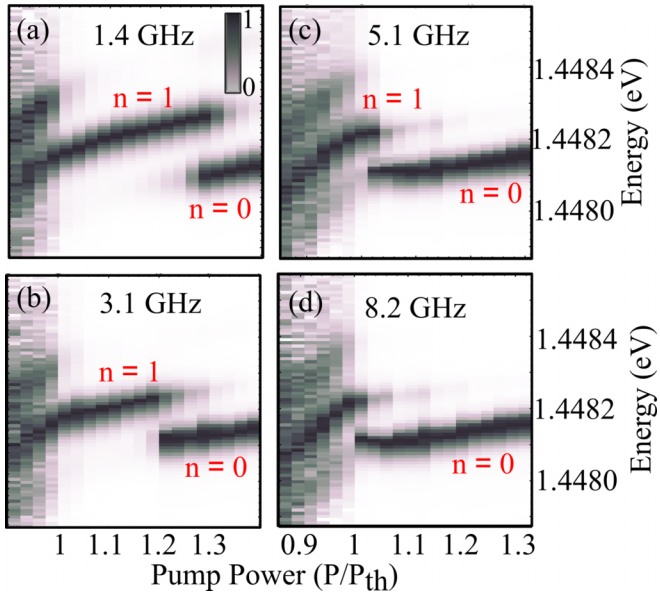

FIG. 2. The condensate normalized spectra as a function of pump power for different rotation frequencies (a) $f = 1.4$ GHz, (b) 3.1 GHz, (c) 5.1 GHz, and (d) 8.2 GHz. The excitation trap diameter is fixed at $d = 14$ μm and n denotes the trap's energy level with $n = 0$ being the ground state.

condensate density. When we increase the diameter of the annular excitation profile to $d = 15.4$ μm and $d = 17.5$ μm, at approximately the same stirring frequency, we observe two and three vortices, respectively, each of the same topological charge $l = 1$, as depicted in Figs. 1(c) and 1(d). The increasing number of vortices with trap size implies that the condensate is shifting its population to higher order trap states as they become available [52–56]. Our experimental results are reproduced with numerical simulations, as shown in Figs. 1(e)–1(g), using the generalized Gross-Pitaevskii equation (see Sec. S3 of the Supplemental Material for details [46]).

To gain a better insight into the physics of the vortex cluster formation, we perform a series of excitation power and rotation frequency scans for each trap size. We start with the smallest trap ($d = 14$ μm) containing just a single vortex. Figure 2 shows the energy-resolved polariton PL measured for different rotation frequencies and variable pump power. Below the condensation threshold (P_{th}), polaritons are broadly distributed across several energy branches corresponding to the confined states of the optical trap. As soon as the threshold is reached, bosonic stimulation forces polaritons to populate a specific energy state accompanied by abrupt linewidth narrowing [13]. At low powers, the condensate is first driven into the branch belonging to the first excited state manifold ($n = 1$), corresponding to the trap's $l = \pm 1$ angular harmonics. In this branch, the condensate can get stirred into a definite direction within a certain rotation frequency interval $|f| \in [1, 4]$ GHz as reported in Ref. [7]. The condensate real-space distribution and dispersion at different stirring frequencies are presented in Sec. S4 of the Supplemental Material [46].

When scanning the pump power, we reveal a transition from the excited to the ground state level ($n = 0$) implying that the condensate vortex eventually destabilizes at higher reservoir densities with condensation shifting into the Gaussian ground state. Interestingly, as we increase the rotation frequency from $f = 1.4$ GHz [Fig. 2(a)] to $f = 8.2$ GHz [Fig. 2(d)], we find that the ground state becomes more dominant over the range of investigated powers. As the pump rotation speed increases, the rotating part of the reservoir smears more out, approaching cylindrical symmetry and restoring the degeneracy between clockwise and anticlockwise polariton currents with no deterministic vorticity forming [7]. Moreover, when the pump power is increased, interactions between the reservoir and the condensate are enhanced, which facilitates energy relaxation of the condensate [53,57,58]. When both effects, fast rotation and high power, are sufficiently strong, they drive the condensate from a vortex state into the vortex-free ground state. This is in sharp contrast to conventional rotating superfluids [1] and BECs [5] as we do not observe an increasing number of vortices at higher rotation frequencies.

We next study a larger rotating trap with $d = 15.4$ μm in which, for $f = -3$ GHz, the condensate intensity distribution [see Fig. 3(a)] features two intensity minima and dominantly occupies the second excited state manifold ($n = 2$) of the trap above threshold [see Fig. 3(b)]. Note that the nonuniform intensity distribution around the circumference of the condensate and its slightly elliptical shape is connected to the imperfections of the annular lasers intensity distribution (see Sec. S2 of the Supplemental Material [46]), making the optical trap slightly elliptical. The two intensity minima correspond to two corotating vortices with $l = -1$ revealed in the real-space phase distribution [see Fig. 3(c)] or $l = +1$ [see Fig. 3(d)] depending on the trap rotation direction (i.e., vortices rotate with the trap). In the Sec. S6 of the Supplemental Material [46] we additionally show the real-space PL and energy-momentum resolved PL of the condensate at other stirring frequencies. We stress that the alignment of the vortices in the cluster is determined by the anisotropy in the net excitation profile or the cavity disorder and is not defined by vortex-vortex interactions like in conventional quantum fluids.

Interestingly, for a similar range of investigated powers as in Fig. 2, we no longer see an abrupt condensate collapse into the ground state energy level in the bigger trap shown in Fig. 3(b). Instead, above $1.3P_{\text{th}}$ the condensate dominantly occupies both the second and ground energy levels at the same time, with a weak population in the first excited level. We find that by fine tuning the size and stirring frequency of the excitation potential, it is possible to create a different energy cascade pattern with the consecutive condensation into different trap levels as a function of pump power. In Sec. S5 of the Supplemental Material [46], we analyze an optical trap with diameter $d = 14.7$ μm that favors the condensation into the first excited level and then the ground level with increasing pump power. As before, the number of stirred vortices is changing on par with the energy state.

Similar to the smaller trap [7], the pair of corotating vortices in the $d = 15.4$ μm trap appear only in a narrow range of stirring frequencies. To reveal this dependence, we analyze the phase distribution of the condensate at different rotation speeds. For each rotation frequency we record 99 excitation shots and obtain corresponding interference patterns of the

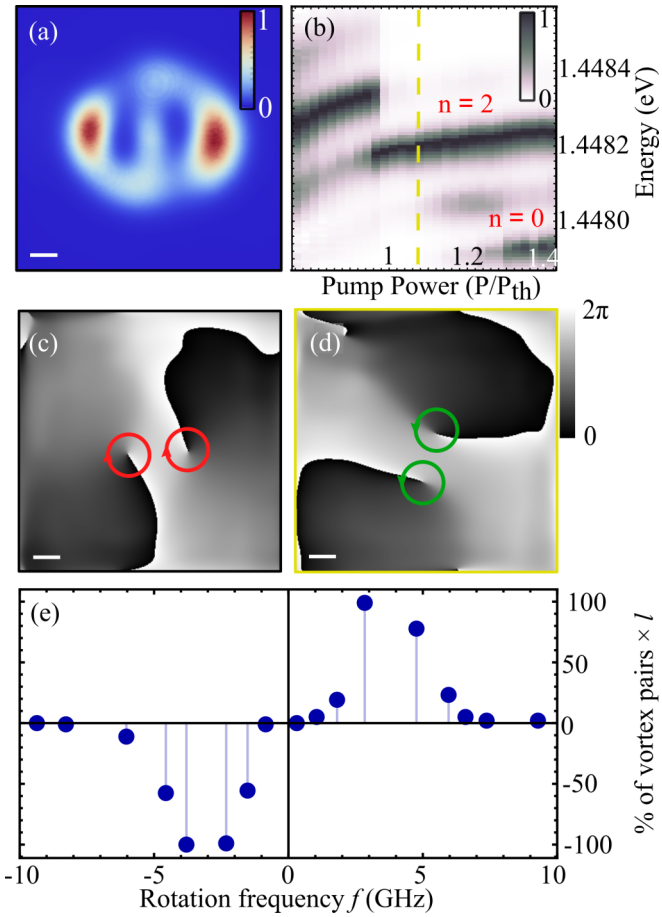

FIG. 3. (a) Real-space condensate intensity distribution for the $d = 15.4$ μm diameter trap rotating at $f = -3$ GHz. (b) The condensate spectrum power dependence ($f = 3$ GHz). The yellow dashed line depicts the pump power corresponding to the retrieved phase profile in panel (d). Condensate phase distribution for (c) $f = -3$ GHz and (d) $f = 3$ GHz. (e) Experimentally extracted distribution of the vortex pair occurrence as a function of stirring frequency. The scale bars in panels (a), (c), and (d) corresponds to 2 μm.

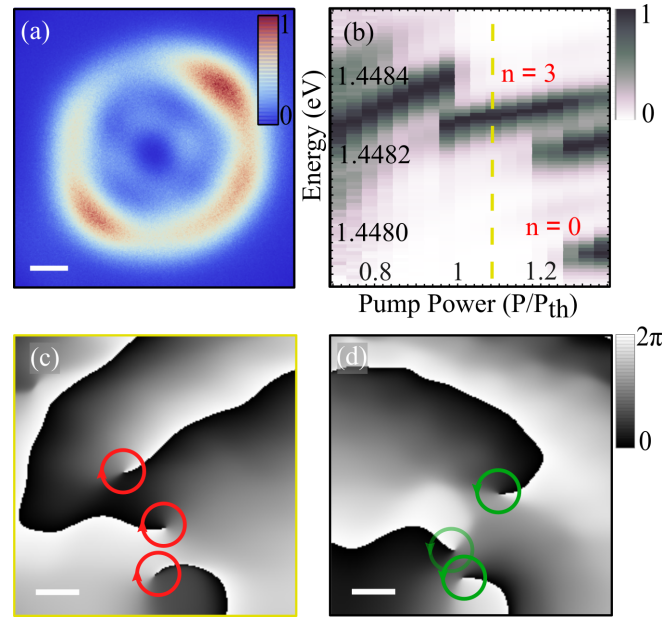

FIG. 4. (a) Real-space condensate intensity distribution for trap diameter $d = 17.5$ μm and rotating at $f = -2$ GHz. (b) Corresponding spectrum power dependence. The yellow dashed line depicts the pump power corresponding to the retrieved phase profile in panel (c). (c), (d) Extracted real-space phase maps for (c) $f = -2$ GHz and (d) $f = 2$ GHz rotation. The scale bars in panels (a), (c), and (d) corresponds to 2 μm.

condensate interfering with the retroreflected displaced copy of itself in a Michelson interferometer. We then extract the azimuthal phase profile at a small fixed distance (2.6 μm) around each of the two phase dislocations in the condensate to check for vorticity and build the histogram presented in Fig. 3(e). To sort out the vortex pairs we calculate the normalized root mean square error (NRMSE) for the experimental phase profile and the ideal vortex [7]. Analyzing 99 condensate phase distribution images for every stirring speed we count only vortices with the NRMSE value less than 0.2. The resulting histogram reflects the percentage of vortex pair occurrences multiplied by the topological charge of the corotating vortices ($l = 1$ or -1) [i.e., normalized average angular momentum of the condensate]. The average angular momentum in Fig. 3(e) follows the sign of the rotation frequencies f meaning that the pair of vortices corotate with the stirring direction. Moreover, the vortices are formed above the critical rotation frequency of $|f| \approx 1.5$ GHz and disappear above $|f| \approx 6$ GHz.

We next increase the trap size even more, to $d = 17.5$ μm. The real-space PL intensity of the condensate in such rotating potential at $f = -2$ GHz is presented in Fig. 4(a). The size of the condensate is increased on par with the optical trap, and just above the threshold, it occupies the third ($n = 3$) excited state manifold of the trap [see Fig. 4(b)]. Similarly to the 15.4 μm trap, the condensation is multimodal for the higher excitation power, with the condensate occupying three energy states above $1.2P_{\text{th}}$. Retrieving the phase of the condensate at $1.1P_{\text{th}}$ we now find a cluster of three corotating vortices with $l = -1$ [see Fig. 4(c)]. Inverting the rotation direction to $f = 2$ GHz makes all vortices flip their topological charges to follow the pump rotation, as shown in Fig. 4(d). As mentioned before, the arrangement of the vortices in the cluster is dictated by nonhomogeneity in the optical potential and cavity disorder. This is also confirmed with the numerical simulation in Figs. 1(f) and 1(g). It is worth noting that unlike the recently observed oscillating vortex cluster [26] created in a static elliptical optical trap, the vortices in a stirred condensate have the same topological charge that does not alter in time.

Finally, for the even larger rotating optical trap ($d = 19$ μm) we observe the condensate with four corotating vortices (see Sec. S7 of the Supplemental Material). Notably, in the experiment, we are able to achieve the confined condensate even in a $d = 37$ μm optical trap as shown Sec. S7 of the Supplemental Material [46]. The condensate, in this case, occupies the $n = 11$ excited manifold of the confining potential and, ergo, could potentially have up to 11 corotating vortices when stirred. However, fine energy splitting in such a large optical trap could influence its phase distribution [26] (at rotating frequency matching the splitting). In this regard,

the study of the larger rotating traps is out of the scope of this work and subject for a separate research.

III. CONCLUSIONS

To sum up, we investigated formation of vortex clusters in nonresonantly optically stirred polariton condensates. We demonstrated that the number of vortices in the clusters scales with the optical trap energy-level (mode) into which polaritons condense. By either changing the size of the pump-induced rotating trap or the excitation power we can adjust the number of observed vortices, with the maximum number achieved in this study being four vortices. We also show that the vortices in the cluster deterministically corotate with the trap stirring direction despite the lack of any phase imprinting coming from the excitation beam in contrast to Refs. [21,59]. Moreover, we find that the energy spectrum of the condensate is rotation frequency-dependent, which is attributed to the finite lifetime of the photoexcited background exciton reservoir responsible for the confinement of the condensate.

We note that presented results do not allow us to make a definitive conclusion on polariton superfluidity, since we do not observe the increasing number of vortices in a cluster with the stirring speed. However, our method could be applied to a much larger unconfined condensate of polaritons [60] to explore vortex-vortex interactions and self-organization between vortices. To achieve this, instead of two opposite Laguerre-Gaussian beams, one beam can be replaced with a flat phase wide-beam Gaussian which would stimulate a larger and denser condensate. This eliminates the strong influence of the trapping potential energy levels (i.e., standing wave interference between polaritons) and potentially give the condensate more freedom to nucleate vortices that self-organize in the same spirit as conservative quantum fluids.

Our findings are relevant to the emerging research direction focused on polariton condensates in time-periodic potentials [7,8,10,61,62]. The redistribution of energy states in the condensate with the stirring speed opens new prospects for the utilization of polaritons as a platform for Floquet engineering [63]. Additionally, advances in all-optical polariton vortex lattices [34] in conjunction with our method can be used to locally manipulate vorticity at individual lattice sites. Finally, the achieved control over polariton flow and state can also benefit the realization of the polariton quantum bits [43,44], as well as sources of structured, coherent, and nonlinear light.

The data presented in this paper are available from the corresponding author upon reasonable request.

ACKNOWLEDGMENTS

The authors acknowledge the support of the European Union's Horizon 2020 program, through a FET Open Research and Innovation Action under the Grant Agreement No. 964770 (TopoLight). H.S. acknowledges the Icelandic Research Fund (Rannís) Grant No. 239552-051. S.A. and I.G. acknowledge the Russian Science Foundation (RSF) (Grant No. 21-72-00088).

[1] E. J. Yarmchuk, M. J. V. Gordon, and R. E. Packard, Observation of stationary vortex arrays in rotating superfluid helium, Phys. Rev. Lett. **43**, 214 (1979).
[2] R. E. Packard and T. M. Sanders, Observations on single vortex lines in rotating superfluid helium, Phys. Rev. A **6**, 799 (1972).
[3] K. W. Madison, F. Chevy, W. Wohlleben, and J. Dalibard, Vortex formation in a stirred Bose-Einstein condensate, Phys. Rev. Lett. **84**, 806 (2000).
[4] M. R. Matthews, B. P. Anderson, P. C. Haljan, D. S. Hall, C. E. Wieman, and E. A. Cornell, Vortices in a Bose-Einstein condensate, Phys. Rev. Lett. **83**, 2498 (1999).
[5] A. L. Fetter, Rotating trapped Bose-Einstein condensates, Rev. Mod. Phys. **81**, 647 (2009).
[6] D. A. Butts and D. S. Rokhsar, Predicted signatures of rotating Bose–Einstein condensates, Nature (London) **397**, 327 (1999).
[7] I. Gnusov, S. Harrison, S. Alyatkin, K. Sitnik, J. Töpfer, H. Sigurdsson, and P. Lagoudakis, Quantum vortex formation in the "rotating bucket" experiment with polariton condensates, Sci. Adv. **9**, eadd1299 (2023).
[8] Y. del Valle-Inclan Redondo, C. Schneider, S. Klembt, S. Höfling, S. Tarucha, and M. D. Fraser, Optically driven rotation of exciton–polariton condensates, Nano Lett. **23**, 4564 (2023).
[9] G. F. Quinteiro Rosen, P. I. Tamborenea, and T. Kuhn, Interplay between optical vortices and condensed matter, Rev. Mod. Phys. **94**, 035003 (2022).
[10] A. V. Yulin, I. A. Shelykh, E. S. Sedov, and A. V. Kavokin, Vorticity of polariton condensates in rotating traps, Phys. Rev. B **108**, 155301 (2023).
[11] A. Kavokin, J. J. Baumberg, G. Malpuech, and F. P. Laussy, *Microcavities* (Oxford University Press, Oxford, UK, 2007).
[12] H. Deng, H. Haug, and Y. Yamamoto, Exciton-polariton Bose-Einstein condensation, Rev. Mod. Phys. **82**, 1489 (2010).
[13] J. Kasprzak, M. Richard, S. Kundermann, A. Baas, P. Jeambrun, J. M. J. Keeling, F. M. Marchetti, M. H. Szymańska, R. André, J. L. Staehli, V. Savona, P. B. Littlewood, B. Deveaud, and L. S. Dang, Bose-Einstein condensation of exciton polaritons, Nature (London) **443**, 409 (2006).
[14] A. Amo, J. Lefrère, S. Pigeon, C. Adrados, C. Ciuti, I. Carusotto, R. Houdré, E. Giacobino, and A. Bramati, Superfluidity of polaritons in semiconductor microcavities, Nat. Phys. **5**, 805 (2009).
[15] G. Lerario, A. Fieramosca, F. Barachati, D. Ballarini, K. S. Daskalakis, L. Dominici, M. D. Giorgi, S. A. Maier, G. Gigli, S. Kéna-Cohen, and D. Sanvitto, Room-temperature superfluidity in a polariton condensate, Nat. Phys. **13**, 837 (2017).
[16] D. Sanvitto, F. M. Marchetti, M. H. Szymańska, G. Tosi, M. Baudisch, F. P. Laussy, D. N. Krizhanovskii, M. S. Skolnick, L. Marrucci, A. Lemaître, J. Bloch, C. Tejedor, and L. Viña, Persistent currents and quantized vortices in a polariton superfluid, Nat. Phys. **6**, 527 (2010).
[17] K. G. Lagoudakis, M. Wouters, M. Richard, A. Baas, I. Carusotto, R. André, L. S. Dang, and B. Deveaud-Plédran, Quantized vortices in an exciton–polariton condensate, Nat. Phys. **4**, 706 (2008).
[18] K. G. Lagoudakis, T. Ostatnický, A. V. Kavokin, Y. G. Rubo, R. André, and B. Deveaud-Plédran, Observation of half-quantum

vortices in an exciton-polariton condensate, Science **326**, 974 (2009).

[19] L. Dominici, G. Dagvadorj, J. M. Fellows, D. Ballarini, M. D. Giorgi, F. M. Marchetti, B. Piccirillo, L. Marrucci, A. Bramati, G. Gigli, M. H. Szymańska, and D. Sanvitto, Vortex and half-vortex dynamics in a nonlinear spinor quantum fluid, Sci. Adv. **1**, e1500807 (2015).

[20] R. Dall, M. D. Fraser, A. S. Desyatnikov, G. Li, S. Brodbeck, M. Kamp, C. Schneider, S. Höfling, and E. A. Ostrovskaya, Creation of orbital angular momentum states with chiral polaritonic lenses, Phys. Rev. Lett. **113**, 200404 (2014).

[21] M.-S. Kwon, B. Y. Oh, S.-H. Gong, J.-H. Kim, H. K. Kang, S. Kang, J. D. Song, H. Choi, and Y.-H. Cho, Direct transfer of light's orbital angular momentum onto a nonresonantly excited polariton superfluid, Phys. Rev. Lett. **122**, 045302 (2019).

[22] X. Ma, B. Berger, M. Aßmann, R. Driben, T. Meier, C. Schneider, S. Höfling, and S. Schumacher, Realization of all-optical vortex switching in exciton-polariton condensates, Nat. Commun. **11**, 897 (2020).

[23] B. Berger, D. Schmidt, X. Ma, S. Schumacher, C. Schneider, S. Höfling, and M. Aßmann, Formation dynamics of exciton-polariton vortices created by nonresonant annular pumping, Phys. Rev. B **101**, 245309 (2020).

[24] T. Gao, G. Li, E. Estrecho, T. C. H. Liew, D. Comber-Todd, A. Nalitov, M. Steger, K. West, L. Pfeiffer, D. W. Snoke, A. V. Kavokin, A. G. Truscott, and E. A. Ostrovskaya, Chiral modes at exceptional points in exciton-polariton quantum fluids, Phys. Rev. Lett. **120**, 065301 (2018).

[25] G. Roumpos, M. D. Fraser, A. Löffler, S. Höfling, A. Forchel, and Y. Yamamoto, Single vortex–antivortex pair in an exciton-polariton condensate, Nat. Phys. **7**, 129 (2011).

[26] K. A. Sitnik, S. Alyatkin, J. D. Töpfer, I. Gnusov, T. Cookson, H. Sigurdsson, and P. G. Lagoudakis, Spontaneous formation of time-periodic vortex cluster in nonlinear fluids of light, Phys. Rev. Lett. **128**, 237402 (2022).

[27] E. S. Sedov, V. A. Lukoshkin, V. K. Kalevich, P. G. Savvidis, and A. V. Kavokin, Circular polariton currents with integer and fractional orbital angular momenta, Phys. Rev. Res. **3**, 013072 (2021).

[28] T. Cookson, K. Kalinin, H. Sigurdsson, J. D. Töpfer, S. Alyatkin, M. Silva, W. Langbein, N. G. Berloff, and P. G. Lagoudakis, Geometric frustration in polygons of polariton condensates creating vortices of varying topological charge, Nat. Commun. **12**, 2120 (2021).

[29] T. Boulier, H. Terças, D. D. Solnyshkov, Q. Glorieux, E. Giacobino, G. Malpuech, and A. Bramati, Vortex chain in a resonantly pumped polariton superfluid, Sci. Rep. **5**, 9230 (2015).

[30] T. Gao, O. A. Egorov, E. Estrecho, K. Winkler, M. Kamp, C. Schneider, S. Höfling, A. G. Truscott, and E. A. Ostrovskaya, Controlled ordering of topological charges in an exciton-polariton chain, Phys. Rev. Lett. **121**, 225302 (2018).

[31] R. Hivet, E. Cancellieri, T. Boulier, D. Ballarini, D. Sanvitto, F. M. Marchetti, M. H. Szymanska, C. Ciuti, E. Giacobino, and A. Bramati, Interaction-shaped vortex-antivortex lattices in polariton fluids, Phys. Rev. B **89**, 134501 (2014).

[32] T. Boulier, E. Cancellieri, N. D. Sangouard, Q. Glorieux, A. V. Kavokin, D. M. Whittaker, E. Giacobino, and A. Bramati, Injection of orbital angular momentum and storage of quantized vortices in polariton superfluids, Phys. Rev. Lett. **116**, 116402 (2016).

[33] G. Tosi, G. Christmann, N. G. Berloff, P. Tsotsis, T. Gao, Z. Hatzopoulos, P. G. Savvidis, and J. J. Baumberg, Geometrically locked vortex lattices in semiconductor quantum fluids, Nat. Commun. **3**, 1243 (2012).

[34] S. Alyatkin, C. Milian, Y. V. Kartashov, K. A. Sitnik, J. D. Topfer, H. Sigurdsson, and P. G. Lagoudakis, All-optical artificial vortex matter in quantum fluids of light, arXiv:2207.01850.

[35] J. Wang, Y. Peng, H. Xu, J. Feng, Y. Huang, J. Wu, T. C. H. Liew, and Q. Xiong, Controllable vortex lasing arrays in a geometrically frustrated exciton-polariton lattice at room temperature, Natl. Sci. Rev. **10**, nwac096 (2023).

[36] G. Nardin, G. Grosso, Y. Léger, B. Pietka, F. Morier-Genoud, and B. Deveaud-Plédran, Hydrodynamic nucleation of quantized vortex pairs in a polariton quantum fluid, Nat. Phys. **7**, 635 (2011).

[37] D. Caputo, N. Bobrovska, D. Ballarini, M. Matuszewski, M. De Giorgi, L. Dominici, K. West, L. N. Pfeiffer, G. Gigli, and D. Sanvitto, Josephson vortices induced by phase twisting a polariton superfluid, Nat. Photon. **13**, 488 (2019).

[38] R. Panico, P. Comaron, M. Matuszewski, A. S. Lanotte, D. Trypogeorgos, G. Gigli, M. D. Giorgi, V. Ardizzone, D. Sanvitto, and D. Ballarini, Onset of vortex clustering and inverse energy cascade in dissipative quantum fluids, Nat. Photon. **17**, 451 (2023).

[39] H. Sigurdsson, G. Li, and T. C. H. Liew, Spontaneous and superfluid chiral edge states in exciton-polariton condensates, Phys. Rev. B **96**, 115453 (2017).

[40] O. Bleu, G. Malpuech, and D. D. Solnyshkov, Robust quantum valley hall effect for vortices in an interacting bosonic quantum fluid, Nat. Commun. **9**, 3991 (2018).

[41] S. L. Harrison, A. Nalitov, P. G. Lagoudakis, and H. Sigurđsson, Polariton vortex chern insulator [invited], Opt. Mater. Express **13**, 2550 (2023).

[42] H. Sigurdsson, O. A. Egorov, X. Ma, I. A. Shelykh, and T. C. H. Liew, Information processing with topologically protected vortex memories in exciton-polariton condensates, Phys. Rev. B **90**, 014504 (2014).

[43] A. Kavokin, T. C. H. Liew, C. Schneider, P. G. Lagoudakis, S. Klembt, and S. Hoefling, Polariton condensates for classical and quantum computing, Nat. Rev. Phys. **4**, 435 (2022).

[44] J. Barrat, A. F. Tzortzakakis, M. Niu, X. Zhou, G. G. Paschos, D. Petrosyan, and P. G. Savvidis, Qubit analog with polariton superfluid in an annular trap, arXiv:2308.05555.

[45] P. Cilibrizzi, A. Askitopoulos, M. Silva, F. Bastiman, E. Clarke, J. M. Zajac, W. Langbein, and P. G. Lagoudakis, Polariton condensation in a strain-compensated planar microcavity with InGaAs quantum wells, Appl. Phys. Lett. **105**, 191118 (2014).

[46] See Supplemental Material at http://link.aps.org/supplemental/10.1103/PhysRevB.109.104503 for details on numerical simulations and additional experimental data.

[47] M. Chen, M. Mazilu, Y. Arita, E. M. Wright, and K. Dholakia, Dynamics of microparticles trapped in a perfect vortex beam, Opt. Lett. **38**, 4919 (2013).

[48] Y. V. Kartashov and D. A. Zezyulin, Rotating patterns in polariton condensates in ring-shaped potentials under a bichromatic pump, Opt. Lett. **44**, 4805 (2019).

[49] A. Askitopoulos, H. Ohadi, A. V. Kavokin, Z. Hatzopoulos, P. G. Savvidis, and P. G. Lagoudakis, Polariton condensation in an optically induced two-dimensional potential, Phys. Rev. B **88**, 041308(R) (2013).

[50] A. Askitopoulos, T. C. H. Liew, H. Ohadi, Z. Hatzopoulos, P. G. Savvidis, and P. G. Lagoudakis, Robust platform for engineering pure-quantum-state transitions in polariton condensates, Phys. Rev. B **92**, 035305 (2015).

[51] S. Alyatkin, J. D. Töpfer, A. Askitopoulos, H. Sigurdsson, and P. G. Lagoudakis, Optical control of couplings in polariton condensate lattices, Phys. Rev. Lett. **124**, 207402 (2020).

[52] A. Dreismann, P. Cristofolini, R. Balili, G. Christmann, F. Pinsker, N. G. Berloff, Z. Hatzopoulos, P. G. Savvidis, and J. J. Baumberg, Coupled counterrotating polariton condensates in optically defined annular potentials, Proc. Natl. Acad. Sci. USA **111**, 8770 (2014).

[53] Y. Sun, Y. Yoon, S. Khan, L. Ge, M. Steger, L. N. Pfeiffer, K. West, H. E. Türeci, D. W. Snoke, and K. A. Nelson, Stable switching among high-order modes in polariton condensates, Phys. Rev. B **97**, 045303 (2018).

[54] X. Ma and S. Schumacher, Vortex multistability and bessel vortices in polariton condensates, Phys. Rev. Lett. **121**, 227404 (2018).

[55] A. V. Nalitov, H. Sigurdsson, S. Morina, Y. S. Krivosenko, I. V. Iorsh, Y. G. Rubo, A. V. Kavokin, and I. A. Shelykh, Optically trapped polariton condensates as semiclassical time crystals, Phys. Rev. A **99**, 033830 (2019).

[56] S. N. Alperin and N. G. Berloff, Multiply charged vortex states of polariton condensates, Optica **8**, 301 (2021).

[57] M. Wouters, T. C. H. Liew, and V. Savona, Energy relaxation in one-dimensional polariton condensates, Phys. Rev. B **82**, 245315 (2010).

[58] E. Estrecho, T. Gao, N. Bobrovska, D. Comber-Todd, M. D. Fraser, M. Steger, K. West, L. N. Pfeiffer, J. Levinsen, M. M. Parish, T. C. H. Liew, M. Matuszewski, D. W. Snoke, A. G. Truscott, and E. A. Ostrovskaya, Direct measurement of polariton-polariton interaction strength in the Thomas-Fermi regime of exciton-polariton condensation, Phys. Rev. B **100**, 035306 (2019).

[59] D. Choi, M. Park, B. Y. Oh, M.-S. Kwon, S. I. Park, S. Kang, J. D. Song, D. Ko, M. Sun, I. G. Savenko, Y.-H. Cho, and H. Choi, Observation of a single quantized vortex vanishment in exciton-polariton superfluids, Phys. Rev. B **105**, L060502 (2022).

[60] D. Ballarini, D. Caputo, C. S. Muñoz, M. De Giorgi, L. Dominici, M. H. Szymańska, K. West, L. N. Pfeiffer, G. Gigli, F. P. Laussy, and D. Sanvitto, Macroscopic two-dimensional polariton condensates, Phys. Rev. Lett. **118**, 215301 (2017).

[61] I. Gnusov, S. Baryshev, H. Sigurdsson, K. Sitnik, J. Töpfer, S. Alyatkin, and P. G. Lagoudakis, Optically driven spin precession in polariton condensates, arXiv:2305.03782.

[62] A. V. Yulin, I. A. Shelykh, E. S. Sedov, and A. V. Kavokin, Spin resonance induced by a mechanical rotation of a polariton condensate, Phys. Rev. B **108**, 045301 (2023).

[63] T. Oka and S. Kitamura, Floquet engineering of quantum materials, Annu. Rev. Condens. Matter Phys. **10**, 387 (2019).